Passive Atmospheric Safety Feature for Small Molten Salt Reactors in Accident Conditions

Brent Edgerton
Mechanical Engineering Department
Brigham Young University

Project Duration: May 29, 2020 – April 23, 2021
Granting Agency: Utah NASA Space Grant Consortium Fellowship, 2020-2021

____

Brent Edgerton

Abstract

This investigation ***aims*** to discover the utility of atmospheric cooling of residual heat in Martian applications (1.5 MW_t). It also considers the possible terrestrial application (45 MW_t) of these concepts. The peculiarities of atmospheric cooling require novel geometric arrangements and material selection. The average convection coefficient is derived and applied to ANSYS Transient Thermal analysis for both terrestrial and Martian environments. This preliminary analysis found that atmospheric cooling is a viable method of Martian passive cooling and may serve as a possible method in terrestrial conditions. **The key finding** of this investigation is that the inclusion of thin SiC conduction panels throughout the salt bodies significantly lowers the thermal gradient of the salt, allowing conduction to serve a greater role in passively cooling molten salt reactors.

1. Introduction

Prerequisite to the establishment of permanent Martian bases, a paradigm shift must occur moving away from the lower power systems reliant on radioactive decay (<1 kW_e) or solar power to higher power systems (>1 MW_e). Highly intricate systems are not feasible for early-stage Martian operation and thus many established active and passive safety systems are not possible in that environment.

This investigation reports on a possible Martian design for a molten salt nuclear reactor that can produce 1.5 MW_t and be passively cooled by atmospheric fluid flow. It also applies the same design considerations to a possible terrestrial 45 MW_t design.

Passive safety can protect astronauts in the event of an accident without requiring them to approach volatile systems until after the thermal event has been contained and the residual heat dispersed. Thus, we will focus our study on the passive cooling post-accident conditions.

2. Design Considerations

2.1 Atmosphere as Fluid

Given that Martian nuclear reactor sites will lack access to the abundant and diverse accident mitigation resources available to terrestrial sites, the atmosphere was chosen as an infinite source of coolant to be used by the core. The Martian atmosphere is 95% CO_2 and will be hereafter treated as pure CO_2 at 6 millibars.

The atmosphere used to cool the core is drawn directly from the external environment of reactor vessel. The gas flows across internal convective surfaces and is immediately expelled into the environment.

2.2 Atmospheric Pressure

While high pressure systems will yield more effective heat transfer across the convective surfaces, the nature of passively cooled reactors prevent the pressurization of the coolant fluid without capturing it in a looped cycle. Such cycles have been rejected in order to explore the feasibility of atmospheric cooling.

Coolant fluid flow is caused by the buoyancy of the hot atmosphere inside the convection channels rising up to be replaced by the cooler external atmosphere from below.

2.3 Internal Free Convection Fins

Convective fins made of Silicon Carbide have been placed throughout the fluid channels in order to increase their surface area and maximize the heat removal. The location and spacing of these fins have been optimized to provide the greatest surface area without significantly slowing the flow velocity.

The convective fins form six rings in the terrestrial model with the center representing an adiabatic core and two rings in the Martian model with the center representing a further third convective region (see Fig. 1).

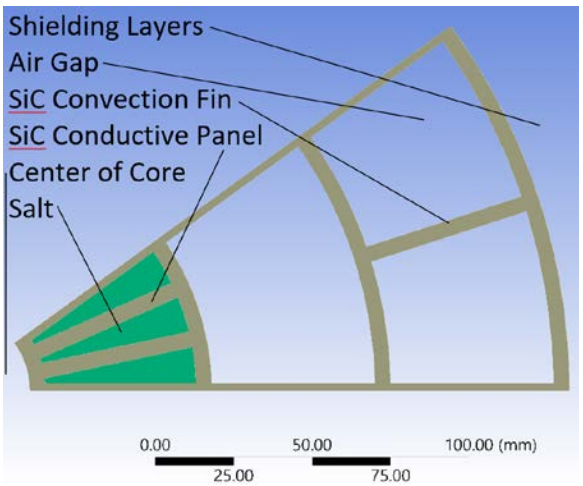

Figure 1. The smaller load requirement on the Martian core meant that less salt was required by volume, allowing for two layers of convective surfaces.

2.4 Fluoride Salt

The uranium fuel has been modeled as being dissolved in the molten salt. FLiNaK has been chosen as the candidate salt for this investigation. The salt has very low thermal conductivity (>1 W/mK)[1] but a very high heat capacity that serves to capture the heat. This salt is held in concentric bodies spaced evenly around the core (see Fig. 2).

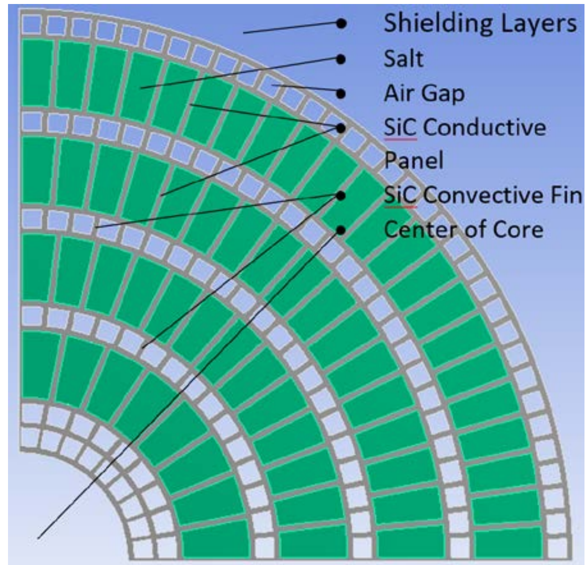

Figure 2. A quarter top view of the terrestrial model's salt bodies is shown in green.

2.5 Conductive Panels

Conductive panels made from SiC have been evenly spaced through the fluoride salt to create thermal "runways," drawing heat away from the center of the salt bodies. These take advantage of the high thermal conductivity offered by SiC and allow nonflowing bodies of molten salt to have their steep thermal gradients moderated (see Appendix Table 1).

Keeping the maximum temperature of the core closer to the conductive surfaces' temperature makes them more efficient and increases the potential power rating of the passive system.

2.6 Active Cooling Features

Active cooling features that would normally be placed throughout the salt bodies in order to cool the reactor and generate electricity during steady operating conditions have not been modeled. Their absence serves to significantly simplify the

[1] Serrano-López. "Molten Salts Database for Energy Applications." 87-102.

core geometry and lends itself to more iterative designing without costing significantly more computational resources.

The absence of these features is justified by the purpose of this model, which is simply to explore the capacity of atmospheric passive cooling. The Hastelloy and aluminum commonly used in cooling pipes have much higher thermal conductivity than the salt and thus their replacement by salt serves as a conservative approximation of the conditions in the core.

3. Silicon Carbide

All structural elements used in this core have been composed of reaction bonded SiC. Materials such as copper were not used because of their low melting points. Future improvements to the design will require the replacement of the SiC convective fins with materials that do not behave as neutron moderators.

The present configuration of the terrestrial core is over-moderated and results in a k_{eff} at initial criticality of 1.92, which is almost supercritical. While negative feedback coefficients and neutron poisons could lower the k_{eff} to operable criticality, replacing structural elements unnecessarily made of SiC with other materials and replacing the salt with active cooling elements will serve a more viable course to bring this core to realistic conditions- a task outside the scope of this present investigation.

3.1 Advantages

Silicon Carbide is chosen as the primary material due to its excellent corrosion characteristics. Molten salts do not dissolve the protective oxide layers of carbides and therefore SiC slows the rate of corrosion, thus avoiding degradation of the material properties and decreasing the chance of structural failure. Corrosion resistance is a requirement for any body in direct contact with the molten salt.

In addition, SiC has a small coefficient of thermal expansion. This limits the thermal strain on the material connecting the hot salt vessel to the relatively cool convective surfaces and the shielding placed outside those.

Silicon has a very small neutron cross section, allowing it to enhance the heat transfer qualities without detracting form the criticality of the core. The carbon serves as a moderator and in the correct proportions can lead to a well-regulated reaction without needing large structural bodies dedicated to moderating the reaction.

3.2 Disadvantages

Silicon carbide is a non-ductile ceramic that is very sensitive to crack propagation and fracture in high tension environments, having a low flexural strength (280 MPa) compared to its compressive strength (2000 MPa).[2] The layered fin structures on the Martian core are potentially susceptible to mechanical failure and a stress analysis has been performed.

4. Fuel Salt

The engineering challenge presented by molten salt reactors in cooling the core comes from the low thermal conductivity of fuel salts. Thermal gradients in the salt do not lead to fluid flow through convection

[2] Li. "Influence of Random Pore Defects on Failure Mode and Mechanical Properties of SiC Ceramics under Uniaxial Compression Using Discrete Element Method." 22270-82.

cycles. The stagnant salt bodies form extremely steep gradients and the localized hot spots are very susceptible to thermal failure.

FLiNaK has been selected as recommended by the Brigham Young University 2020 Nuclear Design Group. The salts defining thermophysical properties are its low thermal conductivity (>1 W/mK) and high specific heat capacity (1900 J/kgK).[3]

FLiBe is frequently selected as the candidate fuel salt by researchers in publications; it has a thermal conductivity (1 W/mK) and specific heat capacity (2400 J/kgK) similar to that of FLiNaK.[4] These salts are representative of the general thermophysical properties of common molten salts.

5. Material Properties Used

Reaction Bonded α-SiC and FLiNaK were selected as the materials to be used in this model (see Appendix Table 1, 2).

6. Thermal Failure

Thermal failure is characterized by the fuel salt exceeding its boiling point at 1570ºC. Boiling reduces the heat transfer capability of the salt and can therefore lead to localized temperature spikes that may melt the structural material. The boiling salt may dissociate from the 233U fuel and create high concentration regions that increase the local power generation which lead to temperature spikes that melt the structural material.

The mechanical failure of the containment vessel due to an increase in internal pressure or temperature will lead to the radioactive isotopes leaking into the air. For the simulation to be conducted safely, the temperature must be held below 1570ºC.

7. Derivation of Convection Coefficient

The posted equations have been drawn from *Fundamentals of Heat and Mass Transfer* by Incropera.[5] The convective fins have been considered as parallel isothermal plates (see Appendix Table 3), assuming the terrestrial and Martian atmospheres behave as ideal gases.

$$\overline{Nu} = \frac{\bar{h}L}{k} \qquad 9.24$$

$$Ra = \frac{gB(T_s - T_\infty)L^3}{\alpha v} \qquad 9.25$$

$$\overline{Nu} = \left(\frac{C_1}{Ra\,S/L} + \frac{C_2}{(Ra\,S/L)^{2/5}}\right)^{-1/2} \qquad 9.46$$

Using a terrestrial S = 0.014 m, we conclude that:

$$Ra = 22.49 \cdot 10^9$$

$$Nu = 26.878$$

$$\bar{h} = 0.936$$

Using a Martian S = 0.052 m, we conclude that:

$$Ra = 12.66 \cdot 10^6$$

$$Nu = 7.516$$

$$\bar{h} = 0.323$$

8. Model Boundary Conditions

Both terrestrial and Martian ANSYS transient thermal simulations were meshed at an

[3] Serrano-López. "Molten Salts Database for Energy Applications." 87-102.

[4] Serrano-López. "Molten Salts Database for Energy Applications." 87-102.

[5] Bergman, T. L.. *Incropera's Principles of Heat and Mass Transfer*, 593-626.

element size of 0.02 m with level 5 resolution. They included convection, surface to surface radiation effects and internal heat generation starting at 45 MW and 1.5 MW, respectively, which decayed according to

$$P = P_o$$
$$t \leq 60\,s$$

and

$$P = P_o(.066)(t-60)^{-.2}$$
$$60\,s < t$$

until the peak temperature visibly declines. The emissivity of the SiC was set at 0.9.

The Martian geometry was given an ANSYS static structural simulation to explore the effects of thermal strain on the fin structures. This geometry had the highest thermal gradient and a structure sensitive to flexural stress. Numerical errors were mitigated by filleting the internal cuts (see Fig. 3).

According to the equation:

$$q = mc\Delta T$$

the terrestrial and Martian t = 60 s temperature should approach 1484°C. The energy generation will fall steeply and the maximum temperature is expected to rise more slowly until the residual heat generation is within the capacity of the convective cooling, at which time the maximum temperature will trend downwards indefinitely.

9. Results

The Martian core behaved as predicted, absorbing and then easily removing the residual heat (see Fig. 4). The small core had nearly no delay to reach the peak temperature after the decay function took effect.

The thermal stresses on the Martian core did not exceed 100 MPa across the body during operating condition (see Fig. 3).

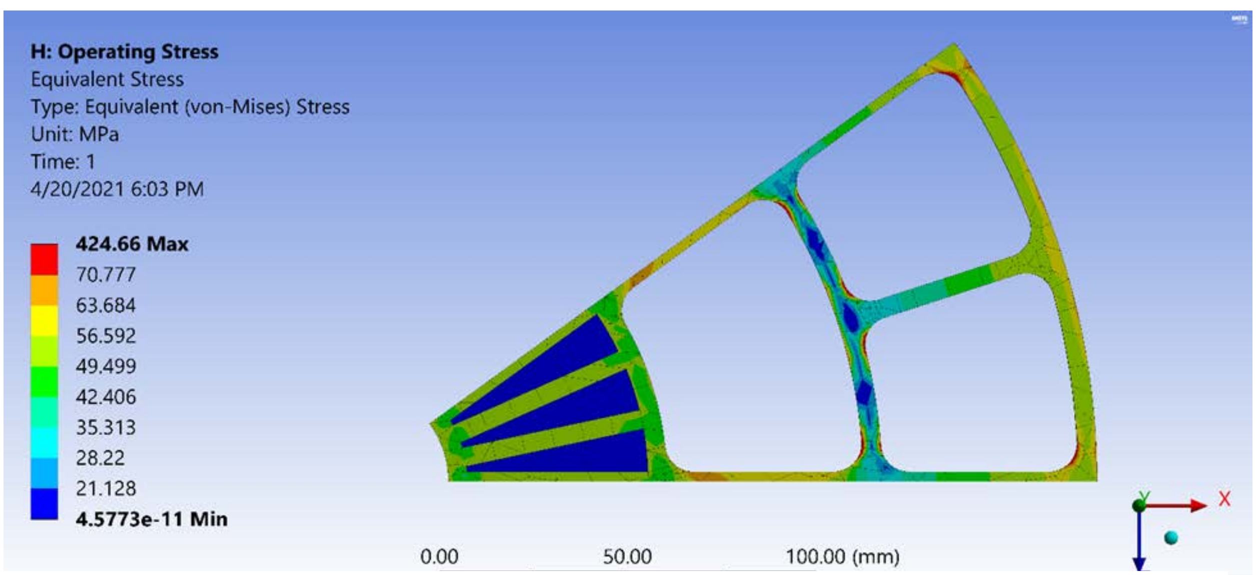

Figure 3. This stress plot shows the thermal stresses imposed on the SiC structure during steady state operation.

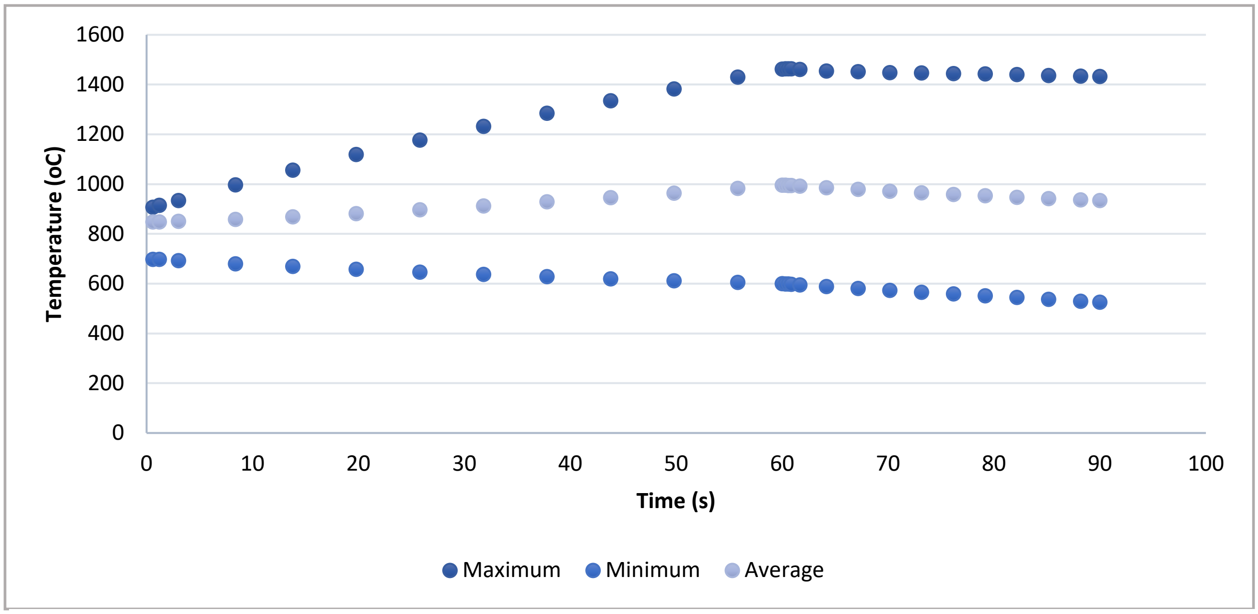

Figure 4. The ANSYS output data for the Martian transient solution. The average can be seen to rise until t = 60 s.

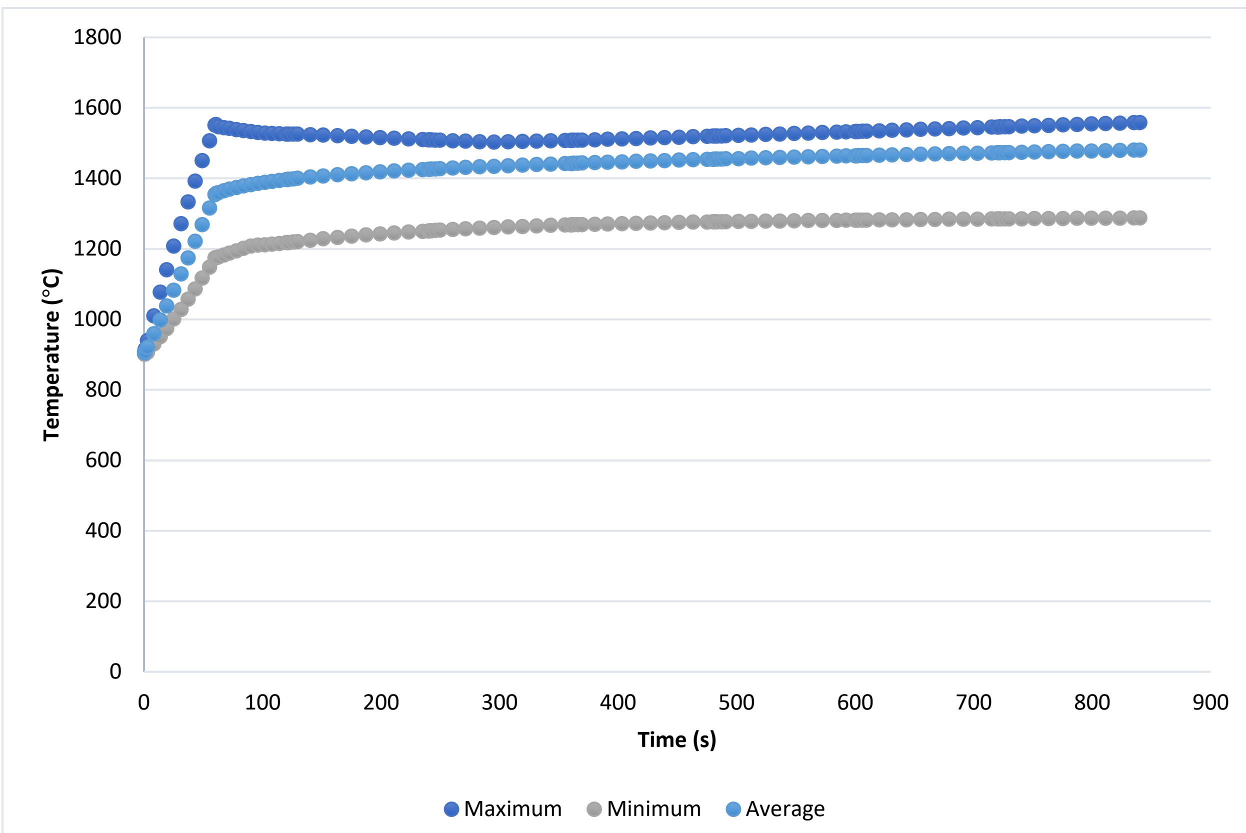

Figure 5. The ANSYS output data for selected salt bodies in the terrestrial transient solution. The average can be seen to rise slowly and the maximum passes above the threshold temperature at t = 667.2 s.

The thermal stresses on the Martian core did not exceed 200 MPa across the body during peak accident conditions (see Appendix Fig. 1). Both stress analysis contained stress concentrations around the edges of the core which can be neglected. The stresses in the center of the core with respect to height reside within a safety factor of 1.85 with respect to the flexural stress.

The terrestrial core was not fully optimized and experienced significant numerical error. The selected salt bodies with the least error were close to 65°C over their true value, giving them a 4.4% error.

The error is generally resolved by t = 300 s and the maximum, minimum, and average increase thereafter. The maximum temperature passes the thermal failure threshold after 667.2 s (see Fig. 5). By 840 seconds the temperature readings have not yet started to decline.

10. Discussion

The Martian core performed better than the terrestrial core because it was loaded with 30 times less power and had significantly more convective and conductive material with respect to the cross-sectional area, regardless of the lower capacity atmosphere. The terrestrial core could not simply be made larger in order to keep the shielding weight within 26 tons. A lower power rating would improve the performance of the terrestrial model and allow this passive method to keep it within 1540°C.

The inclusion of the SiC conduction panels significantly lowers the thermal resistance of the fuel salt bringing the gradient down from over 1000°C to only 230°C (see Fig. 7).

The most striking impact the application of these geometric features makes is the flattening of the thermal gradient (see Fig. 6). The hottest salt regions are prevented from heating past their boiling points while

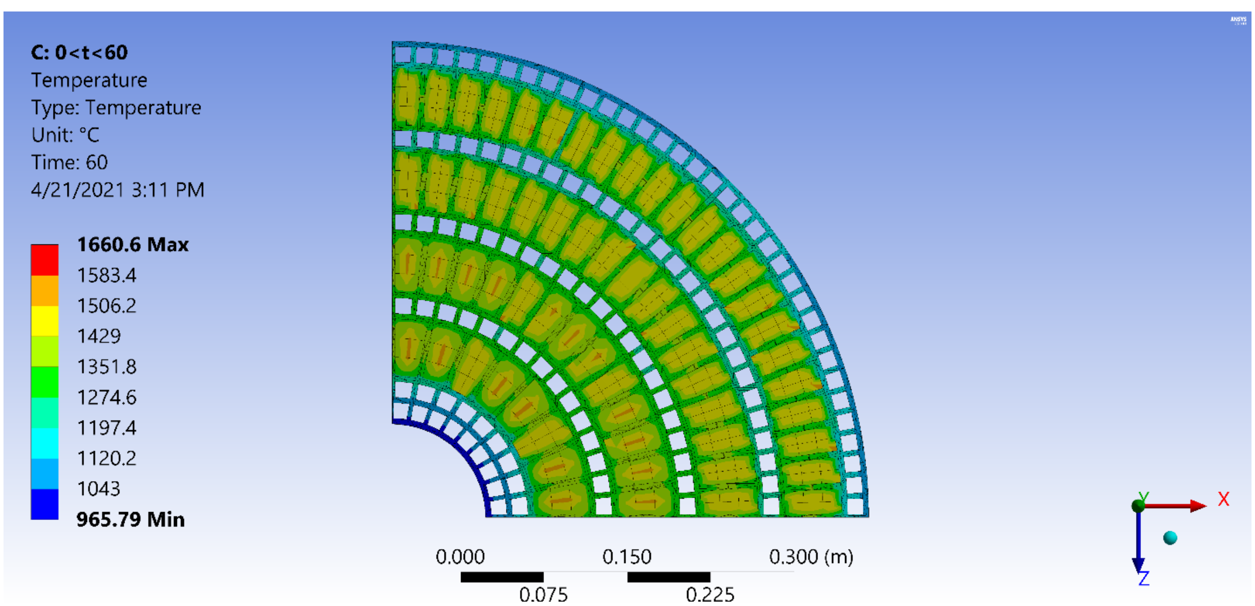

Figure 6. This terrestrial temperature profile shows the ANSYS output at t = 60 s reaching 1660°C, 175°C higher than the true value.

the convective fins are kept as hot as possible to maximize energy removal.

Placing convective channels between the salt bodies is far superior to alternatively placing them around the perimeter of the salt or worse, around the perimeter of the shielding layers. It offers an >430% increase in thermal capacity over submerging the core in water.

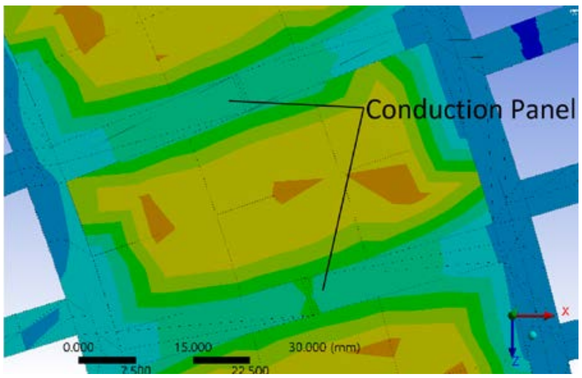

Figure 7. The conduction panels are seen passing through the salt bodies.

11. Challenges to Realistic Solution

11.1 Irradiated Air

Especially terrestrial environments near population centers, irradiated air escaping into the atmosphere poses a challenge to this cooling system. The air must be captured and filtered before being released. Obviously, needing to filter air poses a significant challenge to totally passive cooling systems.

The danger of irradiated cooling fluid is less potent to Martian applications due to the Martian atmosphere already posing a health threat without protective equipment.

11.2 Pipe Blockage

Maintaining a high flow rate is critical to the effectiveness of the convective surfaces. External fires or other damages could pollute the cooling fluid- coating the contact surfaces in soot or preventing all fluid flow. This will destroy the effectiveness of these passive systems. The entry valves must contain filters that will slow the fluid flow rate.

11.3 Delayed Flow

Unless the convective fins are permanently configured to draw heat from the steady state core, the source valves must be opened before the cooling fluid can circulate. The inertial resistance to flow will lead to less energy being removed in the first 60 seconds and cause the average temperatures to rise higher before falling.

12. Conclusion

Atmospheric Cooling is a viable method of passive safety for small molten salt reactors on Martian environments. Atmospheric Cooling is a potential method of passive safety for terrestrial environments if irradiated air can be captured.

Increasing the passive thermal capacity of the reactor is achievable by increasing the rate of convective heat removal and by diluting the residual heat into heat sinks until the convective surfaces match the present level of power generation.

Key finding: the inclusion of SiC conduction panels throughout the salt bodies significantly lowers the temperature difference between the cooling surfaces and the peak salt temperatures. It is the recommendation of this paper that thin SiC panels be inserted throughout the salt bodies to mitigate the primary weakness of molten salts, their conductivity.

Appendix

Table A-1: Selected material properties for Reaction Bonded SiC

Technical Parameter	Unit	SiC
Density	gcm^{-3}	3.03
Coefficient of Thermal Expansion	μC^{-1}	4.1
Young's Modulus	GPa	300
Poisson's Ratio		.16
Tensile Strength	MPa	250 (20°C) 280 (1200°C)
Compression Strength	GPa	2 (20°C)
Thermal Conductivity[6]	$Wm^{-1}C^{-1}$	394 (0°C) 93.3 (500°C) 52.9 (1000°C) 36.92 (1500°C)
Specific Heat, C_p	$Jkg^{-1}C^{-1}$	750

Table A-2: Selected material properties for FLiNaK

Technical Parameter	Unit	FLiNaK
Density	gcm^{-3}	4.1067
Thermal Conductivity[7]	$Wm^{-1}C^{-1}$	.652 (500°C) .733 (550°C) .772 (600°C) .832 (650°C) .927 (700°C) 1.202 (900°C)
Specific Heat, C_p	$Jkg^{-1}C^{-1}$	2500

[6] Nilsson. "Determination of the Thermal Diffusivity and Conductivity of Monocrystalline Silicon Carbide (300-2300 K)." 73-80.

[7] An. "Thermal Conductivity of High Temperature Fluoride Molten Salt Determined by Laser Flash Technique." 872-77.

Table A-3: Selected material properties for air and CO_2.

Technical Parameter	Symbol	Earth (air)	Mars (CO_2)
Fin temperature (°C)	T_s	1500	1500
Fluid temperature (°C)	T_∞	30	0
Acceleration	g	9.81	3.71
Thermal expansion coefficient (°C^{-1})	B	3.32e-3	3.5e-4
Thermal diffusivity (m^2/s)	α	1.117e-4	.015574
Kinematic viscosity (m^2/s)	ν	7.806e-5	4.0474e-5
Height (m)	L	1.6	1.6
Density (kg/m^3)	ρ	.35717	.0036
Conductivity of fluid	K	.05572	.06877

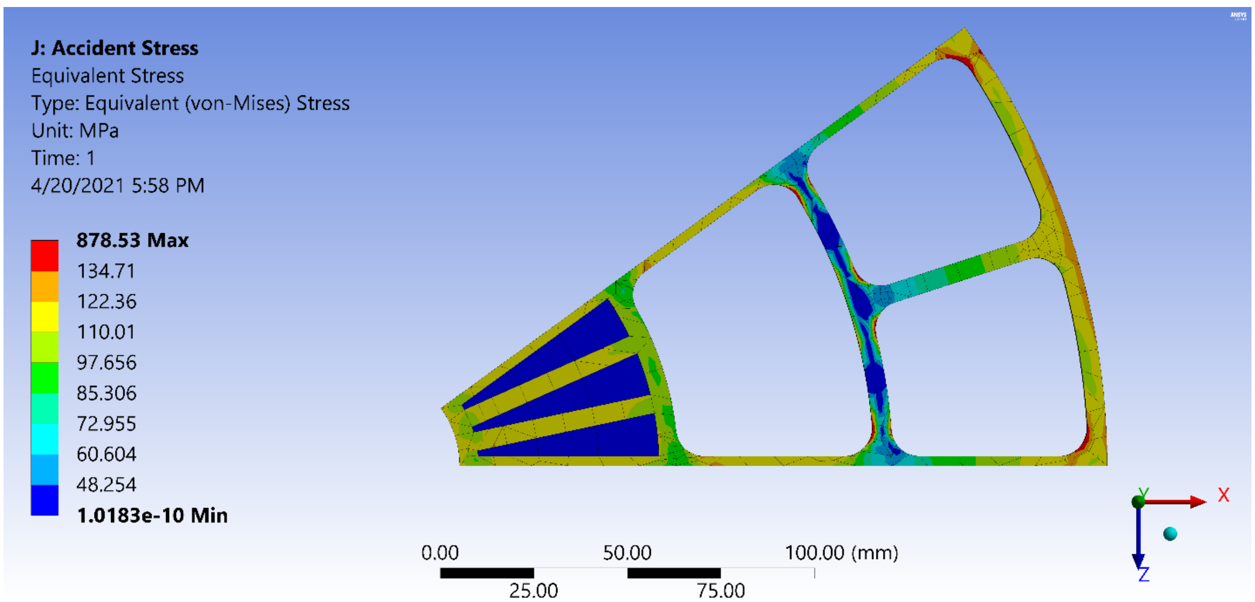

Figure A-1. The accident leads to the steepest thermal gradient and results in higher thermal stress than during the operating state. The central cross section of the core does not exceed 200 MPa.

References

An, Xue-Hui, Jin-Hui Cheng, Hui-Qin Yin, Lei-Dong Xie, and Peng Zhang. “Thermal Conductivity of High Temperature Fluoride Molten Salt Determined by Laser Flash Technique.” *International Journal of Heat and Mass Transfer* 90 (2015): 872–77. https://doi.org/10.1016/j.ijheatmasstransfer.2015.07.042. (Footnote 7)

Bergman, T. L., Adrienne Lavine, David P. DeWitt, Frank P. Incropera, and T. L. Bergman. Essay. In *Incropera's Principles of Heat and Mass Transfer*, 593–626. Hoboken, NJ: Wiley, 2017. (Footnote 5)

Li, Xu, Shengqiang Jiang, Ying Ye, Sisi Liu, Zhiqiang Xu, Yuanqiang Tan, and Dongmin Yang. “Influence of Random Pore Defects on Failure Mode and Mechanical Properties of SiC Ceramics under Uniaxial Compression Using Discrete Element Method.” *Ceramics International* 44, no. 18 (2018): 22271–82. https://doi.org/10.1016/j.ceramint.2018.08.349. (Footnote 2)

Nilsson, Ove, Harald Mehling, Ronny Horn, Jochen Fricke, Rainer Hofmann, Stephan Müller, Robert Eckstein, and Dieter Hofmann. “Determination of the Thermal Diffusivity and Conductivity of Monocrystalline Silicon Carbide (300-2300 K).” *High Temperatures-High Pressures* 29, no. 1 (1997): 73–80. https://doi.org/10.1068/htec142. (Footnote 6)

Serrano-López, R., J. Fradera, and S. Cuesta-López. “Molten Salts Database for Energy Applications.” *Chemical Engineering and Processing: Process Intensification* 73 (2013): 87–102. https://doi.org/10.1016/j.cep.2013.07.008. (Footnote 1, 3, 4)